Structure and Morphology of Fluorocarbon Films Grown by Hot Filament Chemical Vapor Deposition

Kenneth K. S. Lau,[†,§] Jeffrey A. Caulfield,[‡,||] and Karen K. Gleason*,[†]

Department of Chemical Engineering, Massachusetts Institute of Technology, Cambridge, Massachusetts 02139, and Department of Chemical & Bioresource Engineering, Colorado State University, Fort Collins, Colorado 80523

Received June 27, 2000. Revised Manuscript Received July 31, 2000

Hexafluoropropylene oxide (HFPO) flow rate and filament preconditioning time were found to strongly influence the structure and morphology of fluorocarbon films grown by hot filament chemical vapor deposition (HFCVD). The four films discussed in this work all exhibited the vibrational frequencies of linear CF_2 chains, which are also characteristic of bulk poly(tetrafluoroethylene) (PTFE), as shown through Fourier transform infrared spectroscopy (FTIR). The films also incorporated hydroxyl (OH) and carbonyl/carboxyl (CO/COO) groups to varying degrees. Analogous to the behavior of irradiated PTFE, the OH and CO/COO groups may have formed when unterminated chain end radicals reacted with oxygen and water. The surface morphology of the four films, as revealed through atomic force microscopy (AFM), ranged from spherical nodules to anisotropic rodlike grains. An increased aspect ratio of the grains and lower OH incorporation both correlated with the decreased film deposition rate. The hypothesis that long CF_2 chains with a preferred direction of growth are favored by slow deposition would account for both the anisotropy in morphology and the reduction in OH chain ends. An analysis of the chamber effluent supports the proposed mechanism for thermal decomposition of HFPO during HFCVD.

Introduction

Hot filament chemical vapor deposition[1,2] (HFCVD) represents an alternative to plasma-enhanced chemical vapor deposition[3,4] (PECVD) methods for growing fluorocarbon films. In HFCVD, the substrate temperature and gas precursor breakdown temperature are independently controlled, which is a distinct difference from conventional thermal CVD. Specifically, HFCVD enables adsorption-limited reactions to occur on the colder substrate while the hotter filament temperature drives the pyrolytic decomposition of the precursor. The absence of plasma excitation in HFCVD also minimizes the potential structural damage or rearrangement of the film from ion bombardment,[5] X-ray,[6] and electron irradiation.[7]

* To whom correspondence should be addressed. E-mail: kkgleasn@mit.edu.
† Massachusetts Institute of Technology.
‡ Colorado State University.
§ E-mail: klau@mit.edu.
|| E-mail: jeffreyc@colostate.edu.

HFCVD from hexafluoropropylene oxide (HFPO) precursor produces films comprised predominantly of CF_2, as indicated by X-ray photoelectron spectroscopy (XPS).[1,2] Solid-state nuclear magnetic resonance (NMR) spectroscopy shows >97% of the film is comprised of linear $CF_2CF_2CF_2$ chains.[2,8] This is higher in CF_2 content than films deposited by downstream PECVD, which is <90% from XPS.[9,10] The deposition rate for HFCVD can exceed 1 μm/h,[1] which is substantially more rapid than downstream deposition from an HFPO plasma with a rate of 12 nm/h.[10] Thus, HFCVD fluorocarbon films of substantial thickness (>250 nm) can be produced.

Scheme 1 summarizes the potential mechanism for deposition during HFPO HFCVD. HFPO decomposes above 150 °C to generate difluorocarbene (CF_2) and a stable trifluoroacetyl fluoride (TFAcF) gas.[11−13] Gas-phase recombination of two CF_2 diradicals yields tetrafluoroethylene (TFE).[14] Polymerization of TFE into linear CF_2 chains of poly(tetrafluoroethylene) (PTFE) is thermodynamically not very favorable at the conditions of the HFCVD reactor.[15,16] Instead, it is highly

(1) Limb, S. J.; Labelle, C. B.; Gleason, K. K.; Edell, D. J.; Gleason, E. F. *Appl. Phys. Lett.* **1996**, *68*, 2810.
(2) Limb, S. J.; Lau, K. K. S.; Edell, D. J.; Gleason, E. F.; Gleason, K. K. *Plasmas Polym.* **1999**, *4*, 21.
(3) Yasuda, H. *Plasma Polymerization*; Academic Press: Orlando, FL, 1985.
(4) d'Agostino, R., Ed. *Plasma Deposition, Treatment, and Etching of Polymers*; Academic Press: San Diego, CA, 1990.
(5) Wells, R. K.; Ryan, M. E.; Baydal, J. P. S. *J. Phys. Chem.* **1993**, *97*, 12879.
(6) Wheeler, D. R.; Pepper, S. V. *J. Vac. Sci. Technol.* **1982**, *20*, 226.
(7) Clark, D. T.; Brennan, W. J. *J. Electron Spectrosc. Relat. Phenom.* **1986**, *41*, 399.
(8) Lau, K. K. S.; Gleason, K. K. *J. Fluorine Chem.* **2000**, *104*, 119.
(9) Castner, D. G.; Lewis, K. B., Jr.; Fischer, D. A.; Ratner, B. D.; Gland, J. L. *Langmuir* **1993**, *9*, 537.
(10) Butoi, C. I.; Mackie, N. M.; Barnd, J. L.; Fisher, E. R.; Gamble, L. J.; Castner, D. G. *Chem. Mater.* **1999**, *11*, 862.
(11) Sargeant, P. B. *J. Org. Chem.* **1970**, *35*, 678.
(12) Mahler, W.; Resnick, P. R. *J. Fluorine Chem.* **1973**, *3*, 451.
(13) Kennedy, R. C.; Levy, J. B. *J. Fluorine Chem.* **1976**, *7*, 101.
(14) Carlson, G. A. *J. Phys. Chem.* **1971**, *75*, 1625.
(15) Siegle, J. C.; Muus, L. T.; Lin, T.-P.; Larsen, H. A. *J. Polym. Sci., Part A: Polym. Chem.* **1964**, *2*, 391.
(16) Lau, K. K. S.; Gleason, K. K.; Trout, B. L. *J. Chem. Phys.* **2000**, *113*, 4103.

10.1021/cm000499w CCC: $19.00 © 2000 American Chemical Society
Published on Web 09/08/2000

Scheme 1. Pyrolysis and Subsequent Reaction Pathways of HFPO

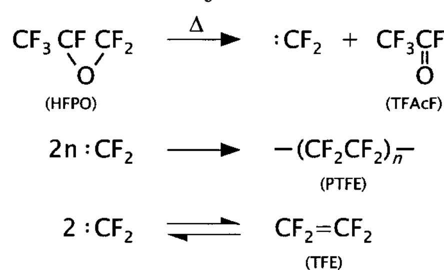

Table 1. Deposition Conditions for HFPO HFCVD Films

	flow rate (sccm)	preconditioning time (min)		flow rate (sccm)	preconditioning time (min)
(a)	15	0	(c)	30	0
(b)	15	15	(d)	30	15

favorable for CF_2 diradicals to undergo such polymerization.[16] It remains to be determined if the polymerization occurs in the gas phase or at the substrate or if polymerization can proceed simultaneously in both locations.

This paper investigates the structure and morphology of HFCVD films prepared under four different CVD conditions using Fourier transform infrared (FTIR) spectroscopy and atomic force microscopy (AFM), respectively. The bulk chemical characterization via FTIR provides a more detailed structural description of the HFCVD fluorocarbon films than from either XPS or solid-state NMR.[2] Furthermore, the bulk characteristics of these relatively thick films (>250 nm) are of great significance for many applications, including low dielectric constant interconnects in microelectronics[17] and biopassivation coatings.[18,19]

Experimental Section

HFCVD was performed using undiluted HFPO ($CF_3CF(O)$-CF_2) (DuPont) at a chamber pressure of 1 Torr. The four deposition conditions, varying only in precursor flow rate and filament preconditioning time, are summarized in Table 1. Preconditioning time refers to the duration of filament heating at the respective process condition prior to actual film deposition. Films were grown on 100-mm-diameter p-type silicon wafers for a total deposition time of 1 h. Each deposition utilized a new 28 AWG Nichrome wire (80% Ni/20% Cr) (Omega Engineering), which was mounted into a filament array and resistively heated to a filament temperature of 500 ± 50 °C. With use of backside water cooling, the substrate temperature was maintained at 21 ± 5 °C. The filament to substrate spacing was 15 mm. Further details of chamber and filament configuration have been described elsewhere.[1,2,20]

Film thickness was measured on a P10 Tencor profilometer. FTIR spectra were acquired under transmission over the range of 400–4000 cm^{-1} on a Nicolet Magna 860 spectrometer with a DTGS KBr detector. A continuous nitrogen purge was used during each acquisition of 64 averages and subsequent spectral

(17) See articles in *MRS Bulletin*; Lee, W. W., Ho, P. S., Eds.; Materials Research Society: Warrendale, PA, 1997; Vol. 22.
(18) Ratner, B. D.; Chikoti, A.; Lopez, G. P. In *Plasma Deposition, Treatment, and Etching of Polymers*; d'Agostino, R., Ed.; Academic Press: San Diego, CA, 1990; pp 463–516.
(19) Panchalingam, V.; Poon, B.; Huo, H. H.; Savage, C. R.; Timmons, R. B.; Eberhart, R. C. *J. Biomater. Sci., Polym. Ed.* **1993**, *5*, 131.
(20) Lau, K. K. S.; Gleason, K. K. *Mater. Res. Soc. Symp. Proc.* **1999**, *544*, 209.

Table 2. Peak Assignments of FTIR Spectra of HFPO HFCVD Films

wavenumber (cm^{-1})	assignment	reference
513/530	CF_2 rock	23, 24
555	CF_2 deformation	23, 24
641/629	CF_2 wag	23, 24
1155	CF_2 symmetric stretch	23, 24
1215	CF_2 asymmetric stretch	23, 24
1708	C=O/COO in CF_xCOO^-	25
3523	OH	26

subtraction removed the background absorption signal from the silicon substrate. The OH/CF_2 ratio was obtained from each spectrum by integrating the broad OH peak centered at 3523 cm^{-1} and dividing by the area of the CF_2 stretches at 1155 and 1215 cm^{-1}.

AFM images were acquired on a Digital Instruments Dimension 3000 under tapping mode with a standard etched silicon tip. Scan areas were 2 × 2 μm, although one film sample with larger grain sizes required a scan area of 50 × 50 μm. For the observed grains, the average and standard deviation of the aspect ratio (length divided by width) were calculated from the measurement of 50–100 grains in each AFM image, sufficient for a statistical representation.[21]

Gas-phase FTIR spectra of the reactor effluent from the final pump stage were taken using a MIDAC I-2000 spectrometer equipped with a ZnSe absorption cell having an optical path length of 1 cm. Spectra were taken of the background with no HFPO flow, of unreacted HFPO, and of the effluent during deposition. To elucidate the gas species present, background-subtracted spectra were regressed using a nonlinear least-squares routine to reference spectra of potential component gases: HFPO, TFAcF, TFE, CO, CO_2, COF_2, CF_4, C_2F_6, C_3F_8, and SiF_4. Further details of the methodology in measurement and analysis, as well as reference spectra, have been published previously.[22]

Results and Discussion

Chemical Bonding. FTIR assignments were based on previous literature[23–26] and are summarized in Table 2. All four FTIR spectra show two strong absorptions at 1155 and 1215 cm^{-1}, assigned as the CF_2 symmetric and asymmetric stretches, respectively (Figure 1). This resolved doublet is also characteristic of bulk PTFE.[27] In contrast, this doublet is generally obscured in the spectra of continuous and pulsed PECVD fluorocarbon films due to overlap with vibrational modes from other bonding configurations, such as CF.[2,28]

All four HFCVD films also give rise to lower wavenumber CF_2 vibrational modes. These peaks in the 500–650-cm^{-1} region are CF_2 rocking, wagging, and deformation modes characteristic of bulk PTFE.[27] In contrast, these low wavenumber modes are absent in both continuous and pulsed PECVD films deposited from HFPO, even when the films have >65% CF_2.[2,29] The

(21) Kim, C. U.; Lee, J. M.; Ihm, S. K. *J. Fluorine Chem.* **1999**, *96*, 11.
(22) Labelle, C. B.; Karecki, S. M.; Reif, R.; Gleason, K. K. *J. Vac. Sci. Technol. A* **1999**, *17*, 3419.
(23) Liang, C. Y.; Krimm, S. *J. Chem. Phys.* **1956**, *25*, 563.
(24) Moynihan, R. E. *J. Am. Chem. Soc.* **1959**, *81*, 1045.
(25) Roeges, N. P. G. *A Guide to the Complete Interpretation of Infrared Spectra of Organic Structures*; Wiley: New York, 1994.
(26) Fisher, W. K.; Corelli, J. C. *J. Polym. Sci., Part A: Polym. Chem.* **1981**, *19*, 2465.
(27) Kobayashi, M.; Sakashita, M.; Adachi, T.; Kobayashi, M. *Macromolecules* **1995**, *28*, 316.
(28) Mackie, N. M.; Dalleska, N. F.; Castner, D. G.; Fisher, E. R. *Chem. Mater.* **1997**, *9*, 349.
(29) Savage, C. R.; Timmons, R. B.; Lin, J. W. *Chem. Mater.* **1991**, *3*, 575.

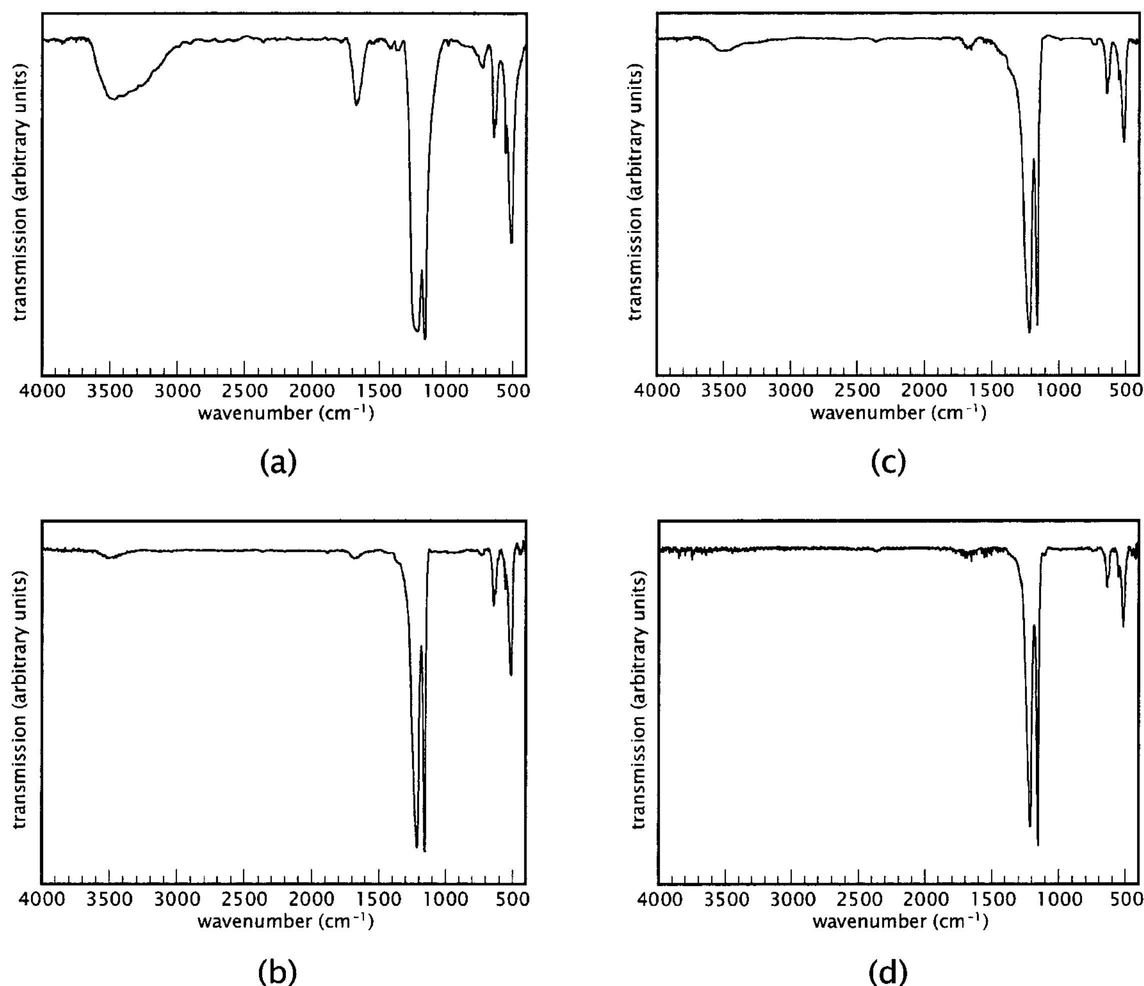

Figure 1. FTIR spectra of HFPO HFCVD films deposited at 1.0 Torr pressure and HFPO flow rates and filament preconditioning times of (a) 15 sccm, 0 min, (b) 15 sccm, 15 min, (c) 30 sccm, 0 min, and (d) 30 sccm, 15 min. Corresponding peak assignments are summarized in Table 2. All spectra feature the vibrational modes of linear CF_2 chain structures characteristic of bulk PTFE. Extraneous OH and CO/COO are attributed to end groups formed from chain end radical reactions with oxygen and water, analogous to irradiated PTFE in air, as shown in Scheme 2.

network structure of these films may hinder such modes.[29] Indeed, solid-state NMR of the pulsed PECVD film with 65% CF_2 reveals cross-linking and branching structures, which may reduce mobility either through steric hindrance or by contribution to the rigidity of the film matrix.[30,31] In contrast, branching or cross-linking structures are absent in solid-state NMR spectra of the HFCVD films.[2,8,20]

In Figure 1, the broad absorption around 3523 cm^{-1} is related to hydroxyl (OH) groups, while carbonyl or carboxyl (CO/COO) groups give rise to a peak centered at 1708 cm^{-1}. The intensities of these peaks vary with the conditions at which the films were deposited. Increasing filament preconditioning time lowers absorption from these oxygen-containing functional groups, as can be seen by comparing Figure 1b to Figure 1a and also by comparing Figure 1d to Figure 1c. Combining filament preconditioning with high HFPO flow rate produces a film with no noticeable OH absorption (Figure 1d). This spectrum also has the most highly resolved doublet in the CF_2 stretch region and is spectroscopically indistinguishable from bulk PTFE.[27]

There are several possible sources of oxygen and hydrogen incorporation. Hydrogen incorporation is most likely from water, either in the chamber background or in the atmosphere. During deposition, oxygen can be derived from the HFPO precursor or from background oxygen and water in the CVD chamber. Postdeposition exposure to atmospheric oxygen and water can also increase oxygen content in the films, a process that has accounted for significant oxygen incorporation in plasma-deposited fluorocarbon films.[32]

Spectroscopic studies of irradiated bulk PTFE after either γ-ray or electron beam irradiation in a vacuum and in air suggest potential pathways for oxygen and hydrogen incorporation in the HFCVD films. Electron spin resonance (ESR) spectroscopy of vacuum-irradiated PTFE has identified relatively stable free radicals, either at the chain end as $-CF_2-CF_2^{\bullet}$ groups or along the chain as $-CF_2-CF^{\bullet}-CF_2-$ groups.[33-37] However, these radicals react readily with oxygen (Scheme 2),

(30) Lau, K. K. S.; Gleason, K. K. *J. Phys. Chem. B* **1997**, *101*, 6839.
(31) Lau, K. K. S.; Gleason, K. K. *J. Phys. Chem. B* **1998**, *102*, 5977.
(32) Horie, M. *J. Vac. Sci. Technol. A* **1995**, *13*, 2490.
(33) Golden, J. H. *J. Polym. Sci.* **1960**, *45*, 534.
(34) Bro, M. I.; Lovejoy, E. R.; McKay, G. R. *J. Appl. Polym. Sci.* **1963**, *7*, 2121.
(35) Siegel, S.; Hedgpath, H. *J. Chem. Phys.* **1967**, *46*, 3904.
(36) Lerner, N. R. *J. Chem. Phys.* **1969**, *50*, 2902.

Scheme 2. Reaction Pathways for the Incorporation of OH and CO/COO End Groups

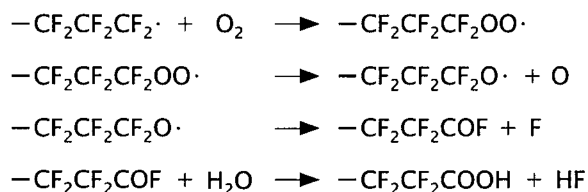

upon subsequent atmospheric exposure or during irradiation in air, to form peroxy radicals, $-CF_2-CF_2OO^{\bullet}$ and $-CF_2-CF(OO^{\bullet})-CF_2-$, respectively.[38,39] Such groups further decompose or react with water to form −COF and −COOH groups, as revealed by FTIR.[40,41]

For HFPO HFCVD, Scheme 1 does not include any termination reaction for CF_2 chain ends. Exposure to oxygen may enable the reaction pathways with oxygen and water as for irradiated PTFE in air. The products would be OH and CO/COO groups, which are indeed observed in the FTIR spectra of the HFCVD films (Figure 1). Regardless of the source, the resulting OH and CO/COO moieties are able to terminate the growth of the linear CF_2 chains. The presence of these groups only at chain ends and not along the chain is consistent with the lack of branching or cross-linking that would otherwise have inhibited the appearance of FTIR modes in the 500−650-cm^{-1} region.[2,29] Thus, high concentrations of these species may indicate lower molecular weight chains. Further, films with a higher OH/CF_2 ratio would contain a greater number of shorter CF_2 chain structures while films with a lower OH/CF_2 ratio would contain a fewer number but longer CF_2 chain structures. It is possible that a lower rate of chain nucleation relative to chain growth would yield fewer but longer chains and consequently fewer chain ends. This point is further discussed in the next section.

It is important to note that oxygen incorporation could occur throughout the bulk of the films. On the basis of the diffusivity (D) of O_2 in PTFE, 3×10^{-8} cm^2/s, derived from the permeability value reported in the literature,[42] the diffusion length ($l = \sqrt{Dt}$) for an exposure time (t) of 60 s is calculated to be 13.4 μm. This far exceeds the typical thickness of deposited films, which is on the order of 100−1000 nm. The time frame between film deposition and subsequent film characterization of over 24 h also far exceeds the exposure time used in the calculation. It is therefore assumed the films would be sufficiently exposed to allow oxygen incorporation in the bulk. The large intensity of the OH absorption in Figure 1a also supports the hypothesis of bulk incorporation.

Film Morphology. Differences in HFCVD film morphology are apparent in Figure 2, which shows AFM images for each of the four films. Films deposited using no filament preconditioning (Figures 2a and 2c) have spherical nodules, while films deposited after 15 min of filament preconditioning (Figure 2b,d) contain elongated rodlike grains. The combination of filament preconditioning with high HFPO flow rate (Figure 2d) results in the highest degree of grain anisotropy. It is interesting that this same pair of conditions minimized oxygen incorporation (Figure 1d). This suggests oxygen incorporation and grain anisotropy may be related effects. Indeed, by plotting the grain aspect ratio and OH/CF_2 ratio as a function of film deposition rate, as shown in Figure 3, the grain aspect ratio decreases while the OH/CF_2 ratio increases with an increasing film deposition rate.

Randomly arranged anisotropic rodlike features have been observed in thin films formed from bulk PTFE latexes.[43] Both spherical and rodlike particles have been observed from conventional emulsion polymerization of TFE to form PTFE.[21,44−47] Studies of the formation of PTFE dispersion particles have revealed distinct nucleation and growth periods during polymerization.[21,48,49] Although the transition from the nucleation to the growth period depends on process conditions, in several cases, it has been found to occur within the first few minutes of polymerization, whether it be in an emulsion polymerization with a surfactant[21] or in an emulsifier-free radiation-induced emulsion polymerization.[49] As growth proceeds, PTFE chains adapt a helical conformation that is highly linear, directional, and rigid with no branching or cross-linking.[50,51] Further, the development of highly extended PTFE chains favor the formation of rodlike grains because, through electron microscopy and X-ray diffraction, rodlike PTFE particles consist of extended chains aligned in the direction of the long axis of the rods.[44,46] Thus, a polymerization process that provides less nucleation would allow greater subsequent growth from these sites and would favor more extended chains with less chain ends and more rodlike grains.

Nucleation and subsequent growth processes may also be occurring during HFCVD from HFPO. The overall decrease in the film deposition rate with increasing HFPO flow rate and filament preconditioning may indicate a reduction in the nucleation rate, which then accounts for the formation of elongated rodlike grains (Figure 3). This also explains the corresponding decrease in film OH because with more extended chains in more anisotropic grains there would be a lower concentration of these end groups (Figure 3).

The importance of preconditioning suggests that the filament plays an active role in the decomposition of HFPO. Indeed, chromium and its oxidized states are known to act as catalysts for the ring opening of

(37) Oshima, A.; Seguchi, T.; Tabata, Y. *Radiat. Phys. Chem.* **1997**, *50*, 601.
(38) Hedvig, P. *J. Chem. Phys.* **1969**, *37*, 479.
(39) Iwasaki, M. *Fluorine Chem. Rev.* **1971**, *5*, 1.
(40) Fischer, D.; Lappan, U.; Hopfe, I.; Eichhorn, K. J.; Lunkwitz, K. *Polymer* **1998**, *39*, 573.
(41) Lunkwitz, K.; Brink, H.-J.; Handte, D.; Ferse, A. *Radiat. Phys. Chem.* **1989**, *33*, 523.
(42) Hintzer, K.; Löhr, G. In *Modern Fluoropolymers*; Scheirs, J., Ed.; Wiley: Chichester, England, 1997; p 253.
(43) Hashimoto, T.; Murakami, Y.; Kawai, H. *J. Polym. Sci., Polym. Phys. Ed.* **1975**, *13*, 1613.
(44) Rahl, F. J.; Evanc, M. A.; Fredericks, R. J.; Reimschuessel, A. C. *J. Polym. Sci., Part A-2* **1972**, *10*, 1337.
(45) Seguchi, T.; Suwa, T.; Tamura, N.; Takehisa, M. *J. Polym. Sci., Polym. Phys. Ed.* **1974**, *12*, 2567.
(46) Chanzy, H. D.; Smith, P.; Revol, J. F. *J. Polym. Sci., Part C: Polym. Lett.* **1986**, *24*, 557.
(47) Luhmann, B.; Feiring, A. E. *Polymer* **1989**, *30*, 1723.
(48) Punderson, J. O. U.S. Patent 3,391,099, 1968.
(49) Suwa, T.; Watanabe, T.; Okamoto, J.; Machi, S. *J. Polym. Sci., Polym. Chem. Ed.* **1978**, *16*, 2931.
(50) Bunn, C. W.; Howells, E. R. *Nature* **1954**, *174*, 549.
(51) Bates, T. W. In *Fluoropolymers*; Wall, L. A., Ed.; Wiley: New York, 1972; pp 451−474.

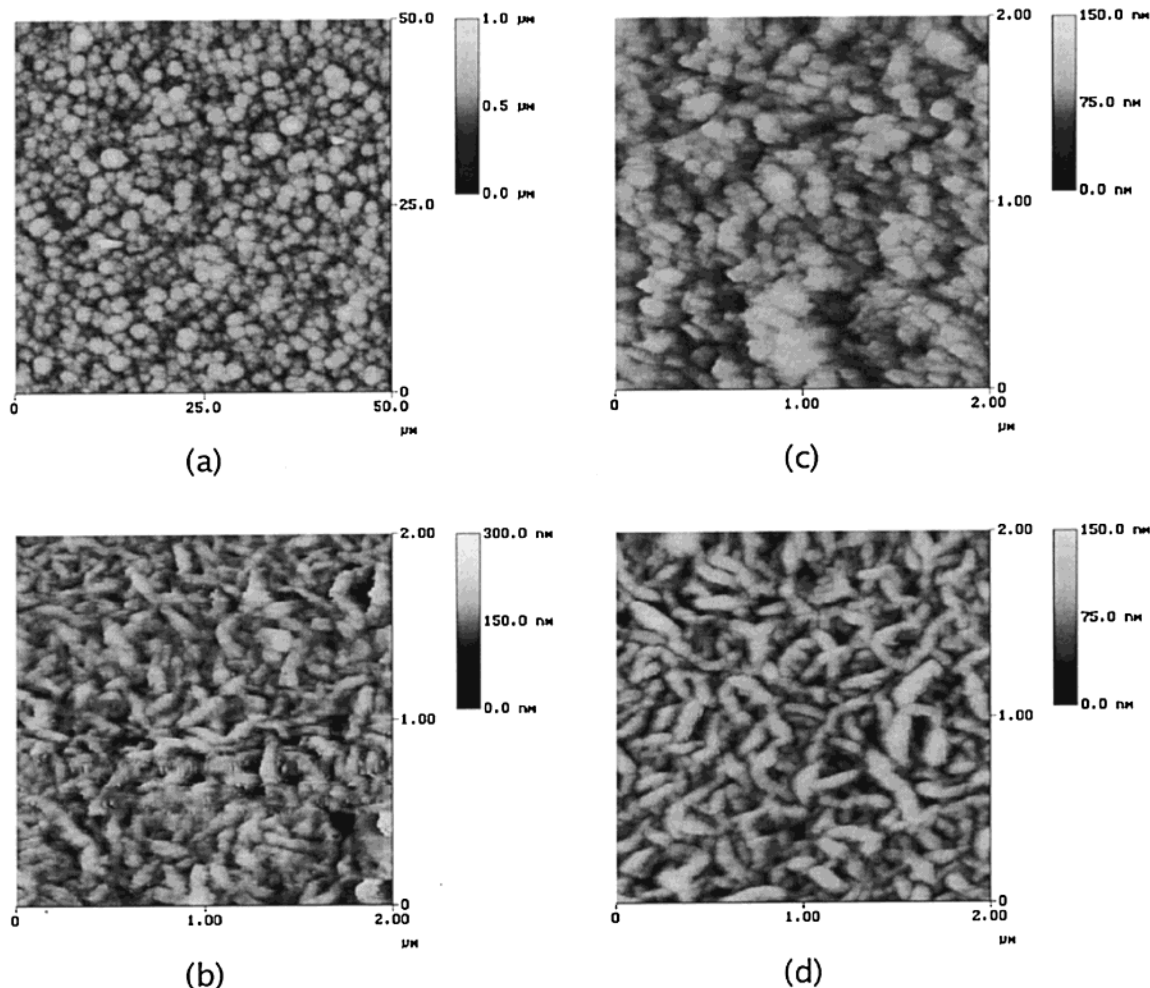

Figure 2. AFM images of HFPO HFCVD films deposited at 1.0 Torr pressure and HFPO flow rates and filament preconditioning times of (a) 15 sccm, 0 min, (b) 15 sccm, 15 min, (c) 30 sccm, 0 min, and (d) 30 sccm, 15 min. Scan areas are 2×2 μm, except for (a), which is 50×50 μm. Morphology ranges from spherical nodules to anisotropic rodlike grains.

epoxides.[52−56] Additionally, the catalytic role of filaments in a HFCVD polycrystalline diamond is well documented.[57,58] A decrease in filament activity may occur through carburization or other poisoning reactions during preconditioning. Further investigation would be required to confirm this proposed effect.

Reactor Effluent. Figure 4a,b shows the FTIR spectra of the reactor exhaust before the filament power was switched on (cold filament) and during deposition when the filament power was on (hot filament), respectively. Spectra shown are for deposition conditions of 1.0 Torr, 15 sccm HFPO, and 15 min of filament preconditioning. As anticipated, Figure 4a is a signature spectrum of pure HFPO.[22] Upon heating the filament, the spectrum changes dramatically (Figure 4b) and spectral regression[22] indicates the presence of only three FTIR active species: unreacted HFPO, the pyrolysis

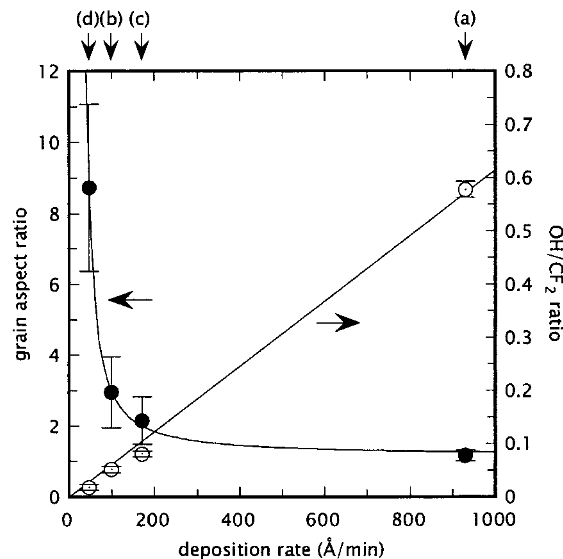

Figure 3. Plot of the grain aspect ratio and OH/CF_2 ratio against the film deposition rate for the four HFPO HFCVD films deposited at conditions given in Table 1. Lower deposition rates result in films with less OH incorporation and more anisotropic grains. The hypothesis of fewer nucleation sites would account for fewer OH end groups, more extended chain growth, and more anisotropic grains.

(52) Martinez, L. E.; Leighton, J. L.; Carsten, D. H.; Jacobsen, E. N. *J. Am. Chem. Soc.* **1995**, *117*, 5897.
(53) Leighton, J. L.; Jacobsen, E. N. *J. Org. Chem.* **1996**, *61*, 389.
(54) Leung, W.-H.; Wu, M.-C.; Chim, J. L. C.; Yu, M.-T.; Hou, H.-W.; Yeung, L.-L.; Wong, W.-T.; Wang, Y. *J. Chem. Soc., Dalton Trans.* **1997**, 3525.
(55) Limberg, C.; Wistuba, T. *J. Org. Chem.* **1999**, *64*, 6169.
(56) Wessjohann, L. A.; Scheid, G. *Synthesis* **1999**, 1.
(57) Moustakas, T. D. *Solid State Ionics* **1989**, *32−33*, 861.
(58) Wolden, C.; Gleason, K. K. *Appl. Phys. Lett.* **1993**, *62*, 2329.

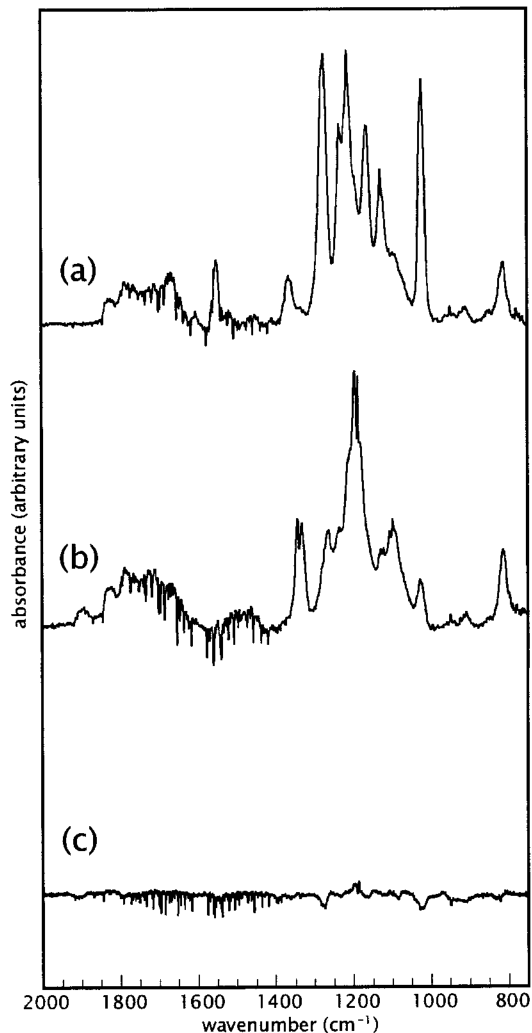

Figure 4. FTIR spectra of gas-phase effluent during HFPO HFCVD: (a) with a cold filament (25 °C) prior to pyrolysis, yields pure HFPO; (b) with a hot filament (500 °C), yields TFAcF, TFE, and HFPO as the only measurable gaseous components; (c) residual spectrum of (b) after regression to a spectral library of pure gases detailed in ref 22, shows good agreement between the raw and regressed spectra. During HFPO pyrolysis, TFAcF is the HFPO decomposition product, TFE is from CF_2 recombination, and HFPO is the remaining unreacted precursor. This supports the anticipated reaction mechanism given in Scheme 1.

product TFAcF, and TFE, the recombination product of CF_2. No measurable amounts of CO, CO_2, COF_2, CF_4, C_2F_6, C_3F_8, or SiF_4 (a measure of free fluorine) were identified. Figure 4c shows the residual spectrum of Figure 4b after regression, demonstrating a good fit between the raw and regressed spectra.

The effluent from HFPO HFCVD contrasts significantly with the effluent species observed during pulsed HFPO PECVD. Pulsed HFPO PECVD gave a variety of gas species in the effluent, including not only HFPO, TFAcF, and TFE but also measurable quantities of CO, CO_2, COF_2, CF_4, C_2F_6, C_3F_6, and C_3F_8.[22] HFCVD provides a much cleaner breakdown route so that pathways in forming byproducts are minimized. Thus, the effluent FTIR results experimentally supports the reaction mechanism for HFCVD given in Scheme 1.

Conclusion

Filament preconditioning and HFPO flow rate strongly influence the structure and morphology of HFCVD fluorocarbon films. All the films displayed the FTIR active vibrational modes of linear CF_2 chain structures, which are also characteristic of bulk PTFE. However, substantial differences in the degree of OH and CO/COO incorporation were observed. These groups could be incorporated via the reactions of unterminated radical chain ends with oxygen and water, analogous to the mechanisms which have been delineated for irradiated PTFE. AFM revealed grain morphologies that ranged from spherical nodules to anisotropic rodlike grains. Filament preconditioning and increased HFPO flow rate decreased film growth rate, decreased oxygen incorporation, and increased grain aspect ratio. The hypothesis of fewer nucleation sites relative to chain propagation would account for the slower film deposition, produce fewer chain ends, and favor the development of rodlike grains. Finally, gas-phase FTIR analysis of HFCVD chamber effluent confirmed that thermal decomposition produces fewer products than plasma decomposition and supports the proposed generation of CF_2 and TFAcF from HFPO.

Acknowledgment. The authors would like to gratefully acknowledge the financial support from both the NSF/SRC Engineering Research Center for Environmentally Benign Semiconductor Manufacturing and the MARCO Focused Research Center on Interconnects funded at the Massachusetts Institute of Technology through a subcontract from the Georgia Institute of Technology. The authors would like to thank Catherine Labelle and Ritwik Chatterjee for their assistance with the gas-phase FTIR setup and measurement. This work also made use of MRSEC Shared Facilities supported by the NSF (DMR-9400334).

CM000499W